



# Cops5 safeguards genomic stability of embryonic stem cells through regulating cellular metabolism and DNA repair

Peng Li<sup>a</sup>, Lulu Gao<sup>a</sup>, Tongxi Cui<sup>a</sup>, Weiyu Zhang<sup>a</sup>, Zixin Zhao<sup>a</sup>, and Lingyi Chen<sup>a,1</sup>

<sup>a</sup>State Key Laboratory of Medicinal Chemical Biology, Collaborative Innovation Center of Tianjin for Medical Epigenetics, Collaborative Innovation Center for Biotherapy, Tianjin Key Laboratory of Protein Sciences, National Demonstration Center for Experimental Biology Education and College of Life Sciences, Nankai University, 300071 Tianjin, China

Edited by Janet Rossant, Hospital for Sick Children, University of Toronto, Toronto, Canada, and approved December 24, 2019 (received for review August 29, 2019)

The highly conserved COP9 signalosome (CSN), composed of 8 subunits (Cops1 to Cops8), has been implicated in pluripotency maintenance of human embryonic stem cells (ESCs). Yet, the mechanism for the CSN to regulate pluripotency remains elusive. We previously showed that Cops2, independent of the CSN, is essential for the pluripotency maintenance of mouse ESCs. In this study, we set out to investigate how Cops5 and Cops8 regulate ESC differentiation and tried to establish Cops5 and Cops8 knockout (KO) ESC lines by CRISPR/Cas9. To our surprise, no Cops5 KO ESC clones were identified out of 127 clones, while three Cops8 KO ESC lines were established out of 70 clones. We then constructed an inducible Cops5 KO ESC line. Cops5 KO leads to decreased expression of the pluripotency marker Nanog, proliferation defect, G2/M cell-cycle arrest, and apoptosis of ESCs. Further analysis revealed dual roles of Cops5 in maintaining genomic stability of ESCs. On one hand, Cops5 suppresses the autophagic degradation of Mth2 to direct cellular metabolism toward glycolysis and minimize reactive oxygen species (ROS) production, thereby reducing endogenous DNA damage. On the other hand, Cops5 is required for high DNA damage repair (DDR) activities in ESCs. Without Cops5, elevated ROS and reduced DDR activities lead to DNA damage accumulation in ESCs. Subsequently, p53 is activated to trigger G2/M arrest and apoptosis. Altogether, our studies reveal an essential role of Cops5 in maintaining genome integrity and self-renewal of ESCs by regulating cellular metabolism and DDR pathways.

Cops5 | genomic stability | cellular metabolism | DNA repair | embryonic stem cells

The unlimited self-renewing capacity and differentiation potential into all types of cells in the body, which is called pluripotency, renders embryonic stem cells (ESCs) a promising donor cell source for regenerative medicine. However, genomic stability and tumorigenicity of ESCs raise safety issues for their clinical applications.

To maintain genome stability, endogenous DNA lesions caused by transcription, replication, and oxidative stresses need to be repaired by various DNA damage repair (DDR) pathways, including base excision repair, mismatch repair, nucleotide excision repair (NER), homologous recombination (HR), and nonhomologous end-joining (NHEJ) (1, 2). Compared with differentiated cells, ESCs have a higher risk to acquire more DNA lesions due to their fast proliferation rate and hyperactive global transcription (3, 4). Yet, mutation frequency in ESCs is lower than that in mouse embryonic fibroblasts (5). At least two strategies, high DDR activities and low levels of reactive oxygen species (ROS), are applied by ESCs to secure the genome integrity (6, 7). To maintain high DDR activities, genes involved in DDR are expressed at higher levels in ESCs than in differentiated cells (8, 9). And ESCs preferentially use HR, rather than NHEJ, to repair DNA double-stranded breaks (DSBs) with high fidelity (10). Moreover, some ESC-specific factors also contribute to efficient DDR. For example, Zscan4, which is

transiently expressed in about 5% of ESCs at a given time, promotes rapid telomere elongation by telomere recombination and regulates genomic stability (11). Induced by genotoxic stress, Fila stimulates the PARP1 activity and relocates from centrosomes to DNA damage sites and mitochondria to regulate DDR and apoptosis (12). Sall4, a pluripotency transcription factor, facilitates the ataxia telangiectasia-mutated activation in response to DSBs (13). To minimize the ROS-induced genomic DNA damage, ESCs produce lower levels of mitochondrial ROS and express higher levels of antioxidants than differentiated cells (14, 15). ESCs predominantly produce ATP through glycolysis, rather than through oxidative phosphorylation (OXPHOS), even though glycolysis is less efficient in energy production (15). The so-called Warburg effect allows sufficient supply of anabolic intermediates for proliferation, as well as minimizing the production of ROS (16). It has been reported that restricting the entry of pyruvate into mitochondria by uncoupling protein 2, together with high levels of hexokinase II and inactive pyruvate dehydrogenase, might rewire the cellular metabolism favoring glycolysis over OXPHOS (17, 18).

The highly conserved COP9 signalosome (CSN) is composed of eight subunits (Cops1 to Cops8). Its most studied function is to regulate protein degradation through suppressing the activity of the cullin-RING-E3 ligases by deneddylation of cullins (19–21). In addition, the CSN is associated with damage specific DNA binding protein 2 (DDB2) and Cockayne syndrome type A protein (CSA) complexes involved in two NER pathways, global

## Significance

Genome integrity is required for clinical applications of pluripotent stem cells. Two major strategies, maintaining low levels of reactive oxygen species (ROS) and high DNA damage repair (DDR) activities, are applied by embryonic stem cells (ESCs) to secure their genomic stability. Here, we demonstrate the pivotal role of Cops5 in safeguarding genome integrity of ESCs. Through regulating the autophagic degradation of Mth2, Cops5 suppresses oxidative phosphorylation and ROS production, thereby reducing endogenous DNA damage. Meanwhile, Cops5 is also involved in maintaining high DDR activities, including nucleotide excision repair, nonhomologous end joining, and homologous recombination, in ESCs.

Author contributions: L.C. designed research; P.L., L.G., T.C., W.Z., and Z.Z. performed research; P.L. analyzed data; and P.L. and L.C. wrote the paper.

The authors declare no competing interest.

This article is a PNAS Direct Submission.

Published under the PNAS license.

<sup>1</sup>To whom correspondence may be addressed. Email: lingyichen@nankai.edu.cn.

This article contains supporting information online at <https://www.pnas.org/lookup/suppl/doi:10.1073/pnas.1915079117/-DCSupplemental>.

First published January 21, 2020.

genome repair (GGR) and transcription coupled repair (TCR), respectively. Knockdown of *COPS5* leads to NER defect (22). A whole-genome RNA interference screening revealed that *COPS1*, *COPS2*, and *COPS4* are required for maintaining the expression of the *OCT4-GFP* reporter in human ESCs, implicating a role of the CSN in pluripotency maintenance (23). However, by knocking down individual CSN subunits, we found that only *Cops2*, but not any other CSN subunits, is essential for the self-renewal and G2/M transition of mouse ESCs (24, 25). Moreover, *Cops5* and *Cops8* null embryos die after embryonic day 7.5, while no *Cops2* null mice survive to embryonic day 7.5 (26–28). These data implicate that *Cops5* and *Cops8* might be involved in late differentiation events, while *Cops2* is essential for the establishment of pluripotency in the inner cell mass.

We set out to investigate how *Cops5* and *Cops8* regulate the differentiation of ESCs and tried to establish *Cops5* and *Cops8* knockout (KO) ESC lines by CRISPR/Cas9. To our surprise, no *Cops5* KO ESC clones were identified out of 127 clones, while three *Cops8* KO ESC lines were established out of 70 clones. We then constructed an inducible *Cops5* KO (*iC5*; *C5* KO) ESC line. *Cops5* KO leads to decreased expression of the pluripotency marker *Nanog*, proliferation defect, G2/M cell-cycle arrest, and apoptosis of ESCs. Further analysis demonstrated that, without *Cops5*, DDR activities are reduced. In addition, loss of *Cops5* accelerates the turnover of *Mtch2* through autophagy, thus altering cellular metabolism toward OXPHOS and enhancing ROS level. Consequently, DNA damages are accumulated in ESCs, and p53 is activated to trigger apoptosis. Altogether, our studies reveal an essential role of *Cops5* in maintaining genome integrity of ESCs by regulating cellular metabolism and DDR pathways.

## Results

***Cops8*, but Not *Cops5*, Can Be Knocked Out in Mouse ESCs.** Aiming to study the roles of *Cops5* and *Cops8* in ESC differentiation, we designed single guide RNAs (sgRNAs) targeting *Cops5* and *Cops8* (Fig. 1 *A* and *B*). The cutting efficiencies of Cas9 at *Cops5*

and *Cops8* loci were about 60 and 56%, as demonstrated by the disruption of the *BsmI* and *HinfI* sites, respectively (Fig. 1 *C* and *D*). Three *Cops8* KO ESC lines were established out of 70 clones. In contrast, no *Cops5* KO ESC line was obtained after screening 127 clones (Fig. 1 *E*). Even though seven clones harboring two disrupted *BsmI* sites in the *Cops5* alleles were identified, none of the seven clones had frameshift mutations in both *Cops5* alleles. These data implied that *Cops5* might be essential for mouse ESCs.

### *Cops5* KO Compromises the Self-Renewal and Differentiation of ESCs.

To directly demonstrate the pivotal role of *Cops5* in pluripotency maintenance of ESCs, we constructed an inducible *Cops5* KO ESC line, using a strategy that we had developed previously (29). A doxycycline-inducible *Cops5* (*iC5*) ESC line was then generated from KH2 cells (30). The sgRNA recognition site in the exogenous inducible *Cops5* gene was mutated to render it resistant to Cas9. Then the endogenous *Cops5* alleles were disrupted in *iC5* ESCs by CRISPR/Cas9 in the presence of doxycycline (Dox), resulting in *iC5*; *C5* KO ESCs. Only a residual amount of *Cops5* remains in *iC5*; *C5* KO ESCs at 48 h after Dox withdrawal, and no *Cops5* is detectable by Western blot at 96 h after Dox withdrawal (Fig. 2 *A*). Notably, depletion of *Cops5* compromises the self-renewal of ESCs, demonstrated by loss of ESC colony morphology, reduced proliferation rate, and colony-forming capacity (Fig. 2 *B–D*). Moreover, *iC5*; *C5* KO ESCs cannot be cultured for more than two passages without Dox. The messenger RNA (mRNA) levels of the pluripotency genes *Nanog*, *Oct4*, and *Sox2* are not altered by *Cops5* KO (Fig. 2 *E*). Yet, *Nanog* protein, but not *Oct4*, is decreased upon *Cops5* KO (Fig. 2 *A*), suggesting that *Cops5* regulates *Nanog* expression posttranscriptionally. With *Nanog* truncation mutants and individual domains fused to luciferase, we found that both N-terminal and C-terminal domains of *Nanog*, but not the Homeobox domain of *Nanog*, mediate the degradation of *Nanog* in *Cops5* KO ESCs (*SI Appendix*, Fig. *S1*). *Cops5* KO also perturbs the expression of differentiation genes, such as *Fgf5*,

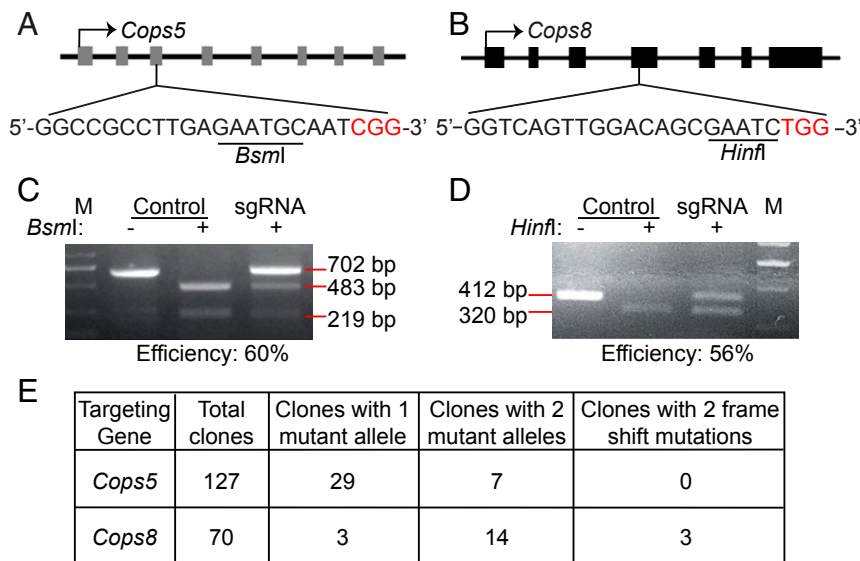


**Fig. 1.** Failure in construction of *Cops5* KO ESC line by CRISPR/Cas9. (*A* and *B*) Schematic illustration of sgRNA design for *Cops5* (*A*) and *Cops8* (*B*). Gray and black rectangles represent the exons of *Cops5* and *Cops8*, respectively. The restriction endonuclease sites in the sgRNA recognition sequences are underlined, and the protospacer-adjacent motifs are shown in red. (*C* and *D*) Cutting efficiency of Cas9 at the *Cops5* (*C*) and *Cops8* (*D*) loci. ESCs were transfected with pX330 plasmids targeting *Cops5* (*C*) and *Cops8* (*D*) or with the pX330 plasmid without an sgRNA insert. Forty-eight hours after transfection, cells were harvested for genomic DNA purification. DNA fragments of 702- and 412-bp around the Cas9 target sites at the *Cops5* and *Cops8* loci were amplified by PCR, respectively. The DNA fragments were digested by *BsmI* or *HinfI*. The intensities of DNA bands were quantified using Image J software, and the cutting efficiency was calculated. (*E*) Genotypes of ESC clones after Cas9 treatment. ESCs were transfected as described in *C* and *D*. Forty-eight hours after transfection, ESCs were treated with trypsin and plated at low density. After 5 to 7 d, individual colonies were picked, expanded, and subjected to genotyping.

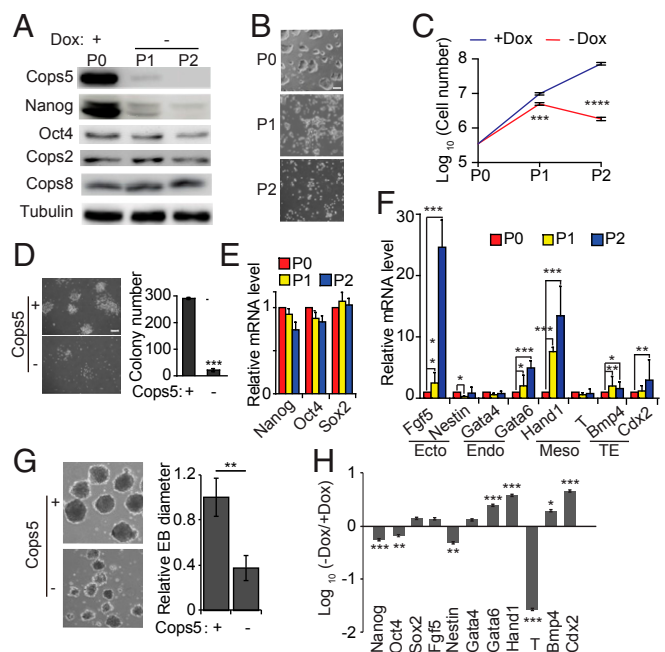


**Fig. 2.** *Cops5* is required for ESC self-renewal and differentiation. (A) *iC5; C5 KO* ESCs cultured with Dox (Passage 0, P0) were switched into medium without Dox for two passages. The protein levels of the pluripotency factors Nanog and Oct4, as well as the CSN subunits, Cops2, Cops5, and Cops8, were measured by Western blot. (B) Colony morphology change upon *Cops5* KO. Phase-contrast images of ESC colonies at each passage are shown. (Scale bar, 100  $\mu$ m.) (C) Growth curves of *Cops5* KO ESCs. *iC5; C5 KO* ESCs were cultured in ESC medium with or without Dox. The cell numbers were counted every passage, and an equal amount of ESCs was plated into tissue culture dishes. (D) Colony forming assay of *iC5; C5 KO* ESCs with or without Dox. (Scale bar, 200  $\mu$ m.) (E) Quantitative RT-PCR was performed to measure the RNA levels of the pluripotency markers *Nanog*, *Oct4*, and *Sox2*. (F) Expression of differentiation genes after *Cops5* KO. (G) *iC5; C5 KO* ESCs were cultured with Dox, and then the cells were used for EB differentiation with or without Dox. (Left) The images of day 4 EBs (40 $\times$  magnification) with or without Dox. The relative diameters of day 4 EBs were measured and plotted (Right). (H) Quantitative RT-PCR analysis of pluripotency and differentiation genes in day 4 EBs, as described in G. \**P* < 0.05; \*\**P* < 0.01; \*\*\**P* < 0.001; \*\*\*\**P* < 0.0001.

*Gata6*, *Hand1*, *Bmp4*, and *Cdx2* (Fig. 2F). All these data suggest an essential role of *Cops5* in ESC self-renewal.

Next, we tested whether *Cops5* is required for the differentiation of ESCs. *iC5; C5 KO* ESCs were cultured with Dox and then were allowed to form embryoid bodies (EBs) in hanging drops with or without Dox. EBs without *Cops5* are smaller than EBs with *Cops5* (Fig. 2G). *Cops5* KO does not block the down-regulation of the pluripotency genes *Nanog*, *Oct4*, and *Sox2*. Rather, it leads to deregulation of differentiation genes, such as elevated expression of *Gata6*, *Hand1*, *Bmp4*, and *Cdx2*, and to reduced expression of *Nestin* and *T* (Fig. 2H). Thus, *Cops5* is also required for EB differentiation of ESCs.

***Cops5* KO Leads to G2/M Arrest and Apoptosis through p53 Activation.**

Given the growth defect of *Cops5* KO ESCs, we analyzed the cell-cycle profile of *iC5; C5 KO* ESCs after Dox withdrawal by propidium iodide staining. G2/M cells, as well as the sub-G1 population (apoptotic cells), are increased upon *Cops5* KO (Fig. 3A). Several key molecular markers for apoptosis, including cleaved Caspase 3, p53, and DNA damage (indicated by  $\gamma$ H2AX and comet assay), are also activated after *Cops5* KO (Fig. 3B and C and SI Appendix, Fig. S2A). To prove that *Cops5* KO activates p53 to induce G2/M arrest and apoptosis, we knocked out *p53* in *iC5; C5 KO* ESCs (SI Appendix, Fig. S2B). *p53* KO partially rescues the

reduced proliferation rate and G2/M arrest caused by *Cops5* KO, whereas *Cops5* KO-induced apoptosis is completely rescued by *p53* KO (Fig. 3D–F). In contrast, the  $\gamma$ H2AX signal, an indicator of DNA damage, is not affected by *p53* KO (SI Appendix, Fig. S2C). These data suggest that *Cops5* KO leads to DNA damage accumulation and subsequently to p53 activation, which in turn induces apoptosis, G2/M arrest, and reduced growth rate.

To address whether the essential role of *Cops5* in ESC self-renewal is dependent on the CSN, we analyzed the effect of *Cops8* KO on ESCs. Both *Cops5* and *Cops8* KO compromise the deneddylation activity of the CSN, indicating disruption of the CSN by *Cops5* or *Cops8* KO (SI Appendix, Fig. S3A). However, except for slightly reduced growth rate, *Cops8* KO ESCs do not have defects in pluripotency marker expression, cell-cycle progression,

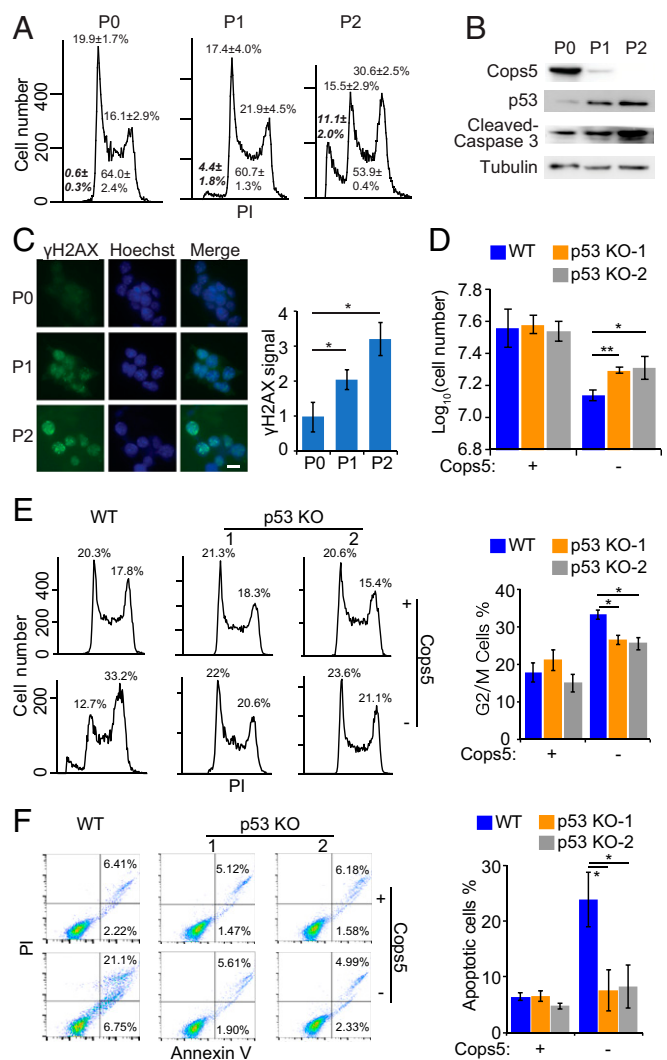


**Fig. 3.** Loss of *Cops5* leads to G2/M arrest and apoptosis through activating p53. (A) Cell-cycle analysis of *iC5; C5 KO* ESCs at different passages after Dox withdrawal. (B) Western blot to detect apoptotic markers, p53, and cleaved Caspase 3 upon *Cops5* KO. (C) Immunofluorescence images of  $\gamma$ H2AX upon *Cops5* KO. (Scale bar, 10  $\mu$ m.) Relative fluorescence intensities of  $\gamma$ H2AX were quantified in around 100 nuclei for each condition. Quantification results were plotted (Right). (D) *iC5; C5 KO* and *iC5; C5 KO; p53 KO* ESCs were cultured in serum/LIF medium with or without Dox for two passages. Cell numbers were counted after two passages, and an equal amount of ESCs were plated into tissue culture dishes. (E and F) Cell-cycle (E) and apoptosis (F) analysis of *iC5; C5 KO* and *iC5; C5 KO; p53 KO* ESCs at different passages after Dox withdrawal. Quantification results are shown on the Right. \**P* < 0.05; \*\**P* < 0.01.

or DNA damage accumulation (*SI Appendix, Fig. S3 B–G*). Moreover, upon differentiation, *Cops8 KO* ESCs fail to activate *T* and *Cdx2*, while *Cdx2* is up-regulated in *Cops5 KO* EBs (Fig. 2H and *SI Appendix, Fig. S3H*). All these data suggest that the CSN-independent function of *Cops5* contributes to pluripotency maintenance of ESCs.

**Cops5 Depletion Impairs DDR Activities.** We then addressed the question how *Cops5 KO* induces DNA damage accumulation. It has been demonstrated that the CSN is associated with DDB2 and CSA complexes, which are involved in two NER pathways, GGR and TCR, respectively. Also, knockdown of *COPS5* in human fibroblasts leads to defects in GGR and TCR (22). Moreover, osteosarcoma U2OS cells with *COPS5* knockdown display HR repair defect (31). Thus, we measured the GGR, TCR, HR, and NHEJ activities in wild-type (WT) and *Cops5 KO* ESCs and found that the GGR, TCR, HR, and NHEJ activities are all reduced in *Cops5 KO* ESCs (Fig. 4). In contrast, *Cops8 KO* does not impair DDR activities (*SI Appendix, Fig. S4 A–D*), arguing that *Cops5*, rather than the CSN, is required for GGR and TCR activities.

It has been reported that, in mouse embryonic fibroblasts and osteosarcoma cells, *Cops5* depletion activates p53, which subsequently suppresses the transcription of *Rad51*, a key gene for HR, and leads to reduced HR activity (31). The working mechanism for *Cops5* to regulate HR in ESCs appears to be different. First, *Rad51* protein, but not *Rad51* mRNA, is reduced in *Cops5 KO* ESCs (*SI Appendix, Fig. S4E*). Second, decreased expression of *Rad51* proteins in *Cops5 KO* ESCs are not completely abolished by *p53 KO* (*SI Appendix, Fig. S4F*). Third, even though *p53 KO* rescue the apoptosis induced by *Cops5 KO*, *p53*

*KO* does not affect DNA damage accumulation in *Cops5 KO* ESCs (*SI Appendix, Fig. S2C*), indicating that p53 is downstream of DNA damage accumulation. Thus, our data suggest that *Cops5 KO* impairs HR activity through down-regulating the *Rad51* protein, independent of p53. Similarly, reduced NHEJ activity in *Cops5 KO* ESCs is likely due to decreased Ku70 protein, a key factor for NHEJ, again independent of p53 (*SI Appendix, Fig. S4 E and F*).

**Cops5 Regulates Cellular Metabolism to Maintain Genome Stability.** *Xpa KO* ESCs, defected in both GGR and TCR, are viable (32). No obvious DNA damage is accumulated in *Xpa KO* ESCs under normal culture conditions (*SI Appendix, Fig. S4G*). In addition, HR and NHEJ activities are only reduced, but not completely abolished, in *Cops5 KO* ESCs. These data imply that reduced DDR activities might not be the only reason for increased DNA damage in *Cops5 KO* ESCs under normal culture conditions. We suspected that DNA damage accumulation in *Cops5 KO* ESCs is due to enhanced endogenous DNA damage, combined with impaired DDR activities. To test this hypothesis, we examined the cellular level of ROS, which is an important oxidative molecule causing endogenous DNA damage. Indeed, *Cops5 KO*, but not *Cops8 KO*, enhances the level of ROS in ESCs (Fig. 5A and *SI Appendix, Fig. S5A*). Consistent with elevated ROS level, glycolysis activity is decreased and OXPHOS activity is enhanced in *Cops5 KO* ESCs, but not in *Cops8 KO* ESCs (Fig. 5B and C and *SI Appendix, Fig. S5 B and C*). Moreover, *Cops5 KO* appears to have a negligible effect on ROS level, glycolysis, and OXPHOS activities in differentiated cells (*SI Appendix, Fig. S5 D–F*). To demonstrate the important role of ROS in elevated DNA damage induced by *Cops5 KO*, we treated ESCs with the reductant *N*-acetylcysteine (NAC). Both  $\gamma$ H2AX immunostaining and a comet assay showed that NAC treatment suppresses DNA damage accumulation in *Cops5 KO* ESCs (Fig. 5D and E).

**Cops5 Regulates Cellular Metabolism through Mch2.** To understand the molecular mechanism of *Cops5* in regulating cellular metabolism, we looked into the list of *Cops5*-interacting proteins identified by coimmunoprecipitation (co-IP) and mass spectrometric analysis (25). We focused on the 49 proteins interacting with *Cops5*, but not with *Cops2* (*Dataset S1*), because the regulation of cellular metabolism by *Cops5* is independent of the CSN. Among these 49 proteins, *Mch2*, a transporter located in the mitochondrial inner membrane, drew our immediate attention. First, the interaction between *Cops5* and *Mch2* was validated by co-IP and Western blot (Fig. 6A and B). Next, we showed that *Mch2* protein, but not its mRNA, decreases upon *Cops5 KO* (Fig. 6C and D). The down-regulation of *Mch2* protein upon *Cops5 KO* is due to autophagic degradation, as the autophagy inhibitor 3-methyladenine (3-MA) restored the level of *Mch2* protein in *Cops5 KO* ESCs (Fig. 6E). We then constructed an *iC5*; *C5 KO* ESC line stably overexpressing *Mch2* (*SI Appendix, Fig. S6A*). *Mch2* overexpression rescues the growth defect of *Cops5 KO* ESCs, as well as reduced glycolysis, enhanced OXPHOS, and elevated ROS level caused by *Cops5 KO* (Fig. 6F–I). More importantly, *Cops5 KO* no longer induces DNA damage accumulation when *Mch2* is overexpressed (Fig. 6J and *SI Appendix, Fig. S6B*). These data indicate that *Mch2* is a key downstream target of *Cops5* in regulating cellular metabolism.

## Discussion

ESCs are able to proliferate infinitely under proper culture condition. For applications of ESCs and their derivatives, such as genetically modified animals and cell replacement therapy, it is necessary to maintain genomic stability of ESCs during the expansion phase. ESCs apply at least two strategies to secure exceptional genomic stability. First, the generation of endogenous DNA damage is minimized through preferentially utilizing glycolysis over OXPHOS to reduce the ROS level (15). Second,

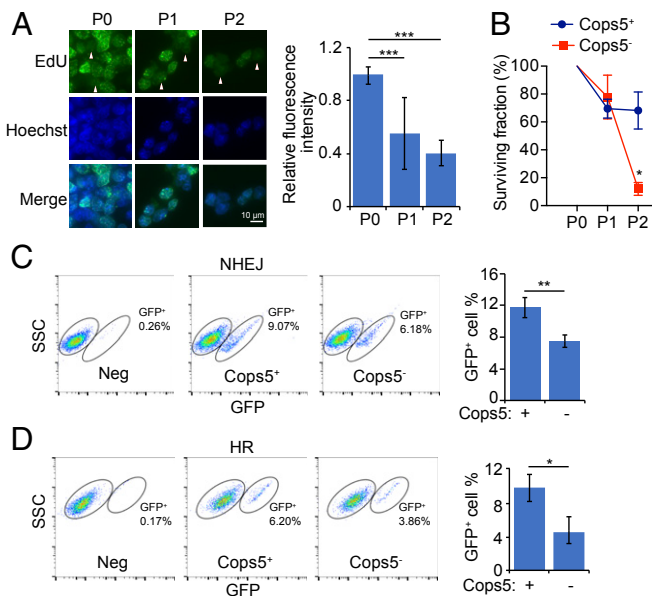


**Fig. 4.** *Cops5 KO* leads to DDR defects in ESCs. (A) *iC5*; *C5 KO* ESCs cultured with (P0) or without Dox for the indicated time (P1, P2) were subjected to GGR assay. Representative images are shown on the *Left*. Triangles indicate non-S-phase cells. (Scale bar, 10  $\mu$ m.) Relative fluorescence intensities of 50 non-S-phase cells were quantified and plotted (*Right*). (B) *iC5*; *C5 KO* ESCs were cultured with or without Dox and exposed to 3  $\mu$ g/mL illudin S for two passages. The surviving fraction was defined as the ratio of live cells with illudin S treatment to live cells without illudin S treatment. (C and D) *iC5*; *C5 KO* ESCs containing NHEJ (C) or HR (D) reporter were cultured with or without Dox for 24 h and then transfected with I-SceI-expressing plasmid. Forty-eight hours after transfection, the percentage of GFP<sup>+</sup> cells was analyzed by flow cytometry. (*Left three panels*) The result of a representative experiment. (*Right*) The quantification result of three independent experiments. \**P* < 0.05; \*\**P* < 0.01; \*\*\**P* < 0.001.

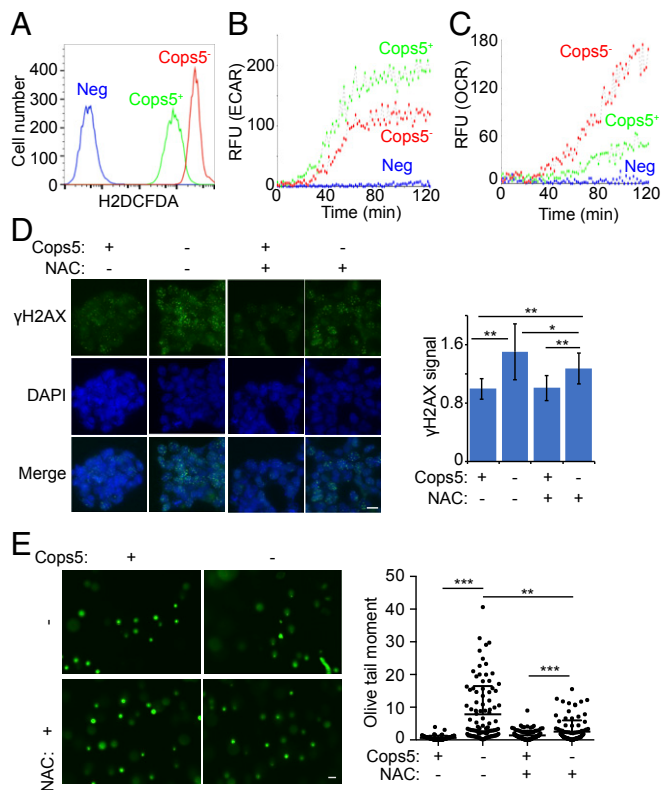


**Fig. 5.** *Cops5* KO alters cellular metabolism and elevates ROS level. (A) Measurement of ROS in *iC5*; *C5* KO ESCs cultured with or without Dox for 48 h. (B) Extracellular acidification rate (ECAR) of *iC5*; *C5* KO ESCs with or without Dox for 48 h. (C) Oxygen consumption rate (OCR) of *iC5*; *C5* KO ESCs with or without Dox for 48 h. (D) *iC5*; *C5* KO ESCs were cultured with or without Dox for 48 h. For the NAC treatment group, 3 mM NAC was added during the 48 h. Representative immunofluorescence images of  $\gamma$ H2AX (three independent experiments) are shown on the *Left*. (Scale bar, 10  $\mu$ m.) Relative fluorescence intensities of  $\gamma$ H2AX were quantified in  $\sim$ 100 nuclei for each condition and plotted (*Right*). (E) Comet assay of *iC5*; *C5* KO ESCs treated as D. (*Left*) The representative images. (Scale bar, 50  $\mu$ m.) Comet tail lengths of 100 cells per sample are quantified (*Right*). \* $P < 0.05$ ; \*\* $P < 0.01$ ; \*\*\* $P < 0.001$ .

high DDR activities are maintained to remove DNA damage efficiently. Both high expression levels of DDR genes and ESC-specific factors, including *Zscan4*, *Filia*, and *Sall4*, contribute to high DDR activities in ESCs (8, 9, 11–13). In this study, we discovered that *Cops5* is involved in both suppressing endogenous DNA damage by ROS and in maintaining high DDR activities to safeguard genome integrity of mouse ESCs. First, *Cops5* ensures the biased energy production by the glycolysis pathway through maintaining the proper expression level of *Mtch2*. Consequently, the generation of ROS is suppressed, thus minimizing endogenous DNA damage caused by ROS. Second, *Cops5* is required for high DDR activities, including NER, HR, and NHEJ, in ESCs. Thus, *Cops5* contributes to genomic stability of ESCs through suppressing endogenous DNA damage and activating DDR activities simultaneously. Without *Cops5*, down-regulated *Mtch2* rewires the cellular metabolism toward OXPHOS, resulting in elevated ROS and endogenous DNA damage. Enhanced endogenous DNA damage, together with impaired DDR activities, leads to accumulation of DNA damage in *Cops5* KO ESCs, which in turn activates p53 and induces G2/M arrest, slow growth rate, and apoptosis (Fig. 7).

We previously reported that *Cops2* is essential for pluripotency maintenance through stabilizing Nanog protein and as a transcriptional corepressor (24). We failed to demonstrate the requirement of *Cops5* in ESC self-renewal by short hairpin RNA

knockdown, most likely due to low efficiency of *Cops5* knockdown. Nevertheless, both *Cops2* and *Cops5* contribute to pluripotency maintenance independent of the CSN. Nanog protein are down-regulated upon *Cops2* knockdown or *Cops5* KO. However, the Homeobox domain of Nanog is required for *Cops2* to promote Nanog protein stability (24), while *Cops5* stabilizes Nanog protein through the N-terminal and C-terminal domains (*SI Appendix*, Fig. S1), suggesting that *Cops2* and *Cops5* regulate Nanog stability through distinct mechanisms. *Cops8* KO ESCs provide further supporting evidences. Both *Cops5* and *Cops8* KO compromise the deneddylation activity of the CSN (*SI Appendix*, Fig. S34). However, except for a slightly reduced growth rate, *Cops8* KO does not affect pluripotency marker expression, cell-cycle

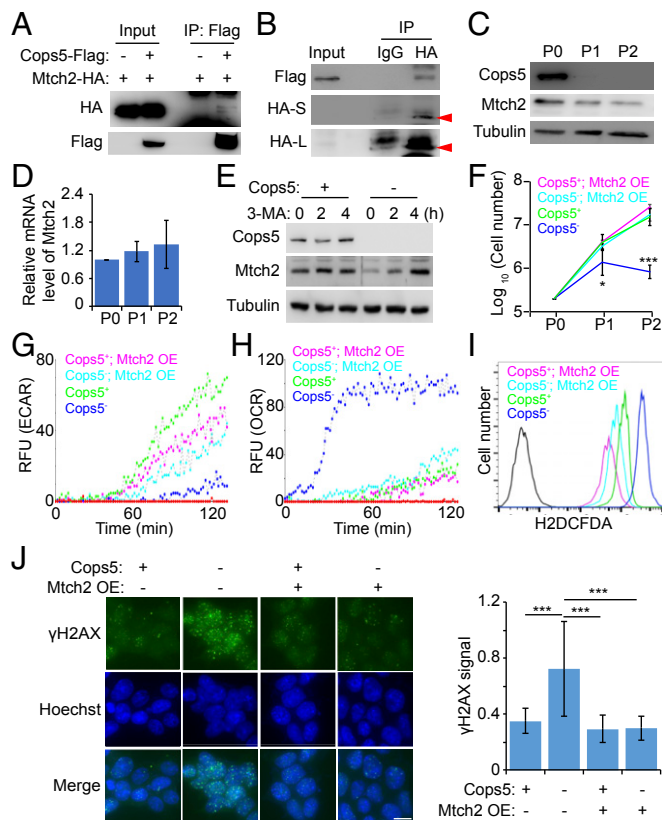


**Fig. 6.** *Cops5* regulates cellular metabolism through *Mtch2*. (A and B) The co-IP experiment to detect the interaction between *Cops5* and *Mtch2*. (A) ESCs with or without stable *Cops5*-Flag expression were transfected with *Mtch2*-HA-expressing plasmid. Forty-eight hours after transfection, cells were harvested for the co-IP experiment using anti-Flag M2 magnetic beads. (B) Cell extracts from ESCs stably expressing *Cops5*-Flag and *Mtch2*-HA were used for the co-IP experiment, using IgG or anti-HA antibody, together with protein G beads. (C and D) *Mtch2* protein (C) and mRNA (D) levels in *iC5*; *C5* KO ESCs at various time points after Dox withdrawal. (E) *iC5*; *C5* KO ESCs were cultured with or without Dox for 48 h and then treated with 5 mM 3-MA for the indicated time. *Mtch2* protein levels in these cells were detected by Western blot. (F) *Mtch2* overexpression rescues the growth defect of *Cops5* KO ESCs. *iC5*; *C5* KO and *iC5*; *C5* KO; *Mtch2* OE ESCs were cultured with or without Dox for two passages. Cell numbers were counted for every passage, and an equal amount of ESCs was plated onto tissue culture dishes. (G) ECAR of *iC5*; *C5* KO and *iC5*; *C5* KO; *Mtch2* OE ESCs with or without Dox for 48 h. (H) OCR of *iC5*; *C5* KO and *iC5*; *C5* KO; *Mtch2* OE ESCs with or without Dox for 48 h. (I) Measurement of ROS in *iC5*; *C5* KO and *iC5*; *C5* KO; *Mtch2* OE ESCs with or without Dox for 48 h. (J) Immunofluorescence images of  $\gamma$ H2AX in *iC5*; *C5* KO and *iC5*; *C5* KO; *Mtch2* OE ESCs with or without Dox for 48 h. (*Left*) Representative immunofluorescence images of three independent experiments. Relative fluorescence intensities of  $\gamma$ H2AX were quantified in  $\sim$ 100 nuclei for each condition and plotted (*Right*). (Scale bar, 10  $\mu$ m.) \* $P < 0.05$ ; \*\*\* $P < 0.001$ .

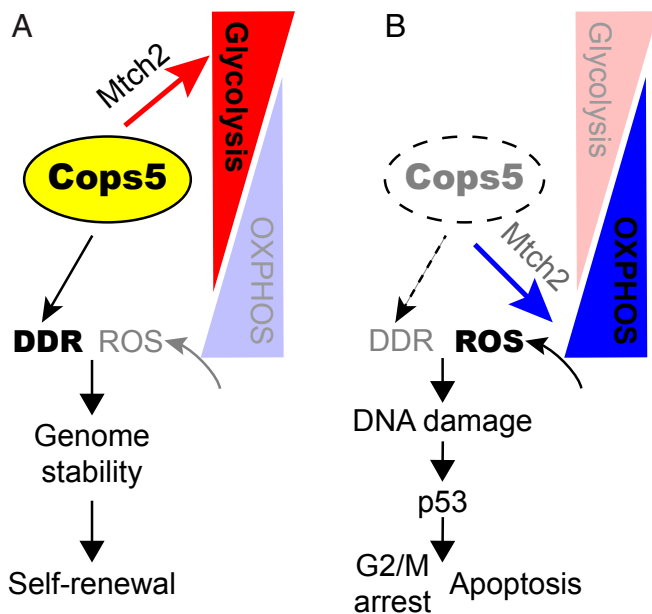


**Fig. 7.** A working model for Cops5 to regulate genomic stability of ESCs. (A) Cops5 promotes cellular metabolism toward glycolysis through maintaining Mch2 expression, thereby suppressing ROS production. In addition, high DDR activities, which are dependent on Cops5, together with low ROS, ensure the genomic stability and self-renewal of ESCs. (B) Without Cops5, a reduced level of Mch2 rewires cellular metabolism to OXPHOS, leading to elevated ROS. Enhanced ROS level, as well as compromised DDR activities, cause DNA damage accumulation in ESCs, which in turn activates p53, G2/M arrest, and apoptosis.

progression, or DNA damage accumulation in ESCs (*SI Appendix, Fig. S3 B–G*). Moreover, *Cops8* KO does not affect DDR activities, cellular ROS level, glycolysis, and OXPHOS activities (*SI Appendix, Fig. S4 A–D*). All these data suggest that CSN-independent function of Cops5 contributes to pluripotency maintenance and genomic stability of ESCs.

Our data show that *Cops5* KO reprograms the cellular metabolism toward OXPHOS through down-regulating Mch2. However, there are conflicting results regarding Mch2 in metabolism regulation. *Mch2* KO enhances glycolytic flux and suppresses OXPHOS in ESCs (33). In contrast, loss of *Mch2* in hematopoietic stem cells (HSCs) and skeleton muscle cells promotes the metabolic switch from glycolysis to mitochondrial OXPHOS (34, 35). Our data are consistent with the metabolic regulatory function of Mch2 in HSCs and skeleton muscle cells, despite that we studied Mch2 in ESCs. Down-regulation of Mch2 in our study and *Mch2* KO in the work by Bahat et al. (33) might account for the opposite effects in regulating metabolic switch. Consistent with this note, knockdown of *Mch2* with small interfering RNA in ESCs leads to down-regulation of glycolysis and elevation of OXPHOS (*SI Appendix, Fig. S6 C–F*). Alternatively, the difference in ESC culture conditions might contribute to the seemingly conflicting observation. We cultured ESCs in the presence of leukemia inhibitory factor (LIF) and serum, while *Mch2* KO ESCs were cultured in 2i/LIF and serum-free condition.

*Cops5* KO down-regulates Mch2 through autophagic degradation. Yet, the detailed mechanism of how Cops5 regulates autophagic degradation of Mch2 remains unclear. Cops5 is a metalloprotease with deneddylation and deubiquitination activities (22). In addition to its well-known role in proteasomal degradation, ubiquitin also serves as a key signal for selective autophagy (36, 37). Thus, it is possible that Cops5 regulates the autophagy of Mch2 by deubiquitinating Mch2. In addition, it has been shown that Cops5 regulates autophagy via the ERN1 and mTOR pathways in goat endometrial epithelial cells (38). Given that Cops5 interacts with

the mitochondrial protein Mch2, the possibility is raised that Cops5 regulates mitophagy or, even more specifically, the autophagy of Mch2. Interestingly, mitophagy plays an important role in metabolic switch and cell-fate change (39, 40). Thus, further investigation of how Cops5 regulates the autophagic degradation of Mch2 might shed light on metabolic regulation and cell-fate determination of ESCs.

## Materials and Methods

**Cell Culture and Transfection.** D3 and KH2 ESCs were cultured in ESC medium which consists of 15% fetal bovine serum (FBS) (HyClone), 85% Dulbecco's Modified Eagle Media (DMEM) (high-glucose DMEM, Gibco), 2 mM L-glutamine, 5,000 units/mL penicillin and streptomycin, 0.1 mM nonessential amino acids (Invitrogen), 0.1 mM  $\beta$ -mercaptoethanol (Sigma), and 1,000 units/mL LIF (Millipore).

To establish the *iC5* ESC line, KH2 ESCs were transfected with pBS31-*Cops5m* and pCAGGS FLPe using lipofectamine 3000 (Invitrogen) (30). After 10-d of hygromycin selection, individual colonies were picked up and validated by genotyping. To induce the expression of exogenous *Cops5* gene, 1  $\mu$ M Dox was added into medium. To knockout *Cops5* or *Cops8*, pX330 plasmids targeting *Cops5* or *Cops8* were transfected into ESCs using lipofectamine 3000. Two days after transfection, ESCs were plated down at low density to allow the formation of colonies from single cells. Five to seven days later, individual colonies were picked up and subjected to further culture and analysis.

**GGR Assay.** GGR assay was performed as described elsewhere (41). Coverslips were placed into a 24-well plate and coated with gelatin in advance. ESCs ( $1 \times 10^5$ ) were plated into each well and cultured to 50% confluence. Cells were washed with phosphate-buffered saline (PBS) and irradiated with 5 J/m<sup>2</sup> ultraviolet (UV) light for 5 s. Immediately after UV irradiation, cells were immediately incubated with 5-ethynyl-2'-deoxyuridine (final concentration 10  $\mu$ M, Invitrogen, C10637) in serum-free DMEM for 4 h at 37 °C. After three washes with PBS, cells were fixed and permeabilized in buffer 1 (2% paraformaldehyde; 0.5% Triton-X; 0.3 M sucrose; diluted in PBS) on ice for 20 min, followed by three washes with 10% FBS in PBS for 5 min each. Cells were blocked with PBS containing 10% FBS for 30 min at room temperature. After aspirating PBS, 1  $\mu$ L of 2.5 mM Alexa Fluor 488-azide and 100  $\mu$ L buffer 2 (4 mM CuSO<sub>4</sub>; 10 mM sodium ascorbate; 50 mM Tris-HCl, pH 7.3) were mixed and added to the cells. After a 1-h incubation at room temperature, cells were washed three times with PBST (0.05% Tween 20) for 5 min each. Hoechst 33342 (5  $\mu$ g/mL) diluted with PBS was added to the cells. After a 20-min incubation at room temperature, cells were fixed with 3.7% formaldehyde for 20 min. Images were captured by Zeiss Axio-Imager Z1 fluorescence microscope and analyzed by Image J software.

**TCR Assay.** TCR assay was performed as described elsewhere (32). Cells ( $2.5 \times 10^5$ ) were plated into each well of a six-well plate, cultured with or without Dox. Simultaneously, 3  $\mu$ g/mL Illudin S (Santa Cruz, SC-391575) was added to the medium for the experimental group. At passages 1 and 2, cells were harvested, and live cells were counted under a microscope after Trypan blue staining.

**Measurement of NHEJ and HR.** The NHEJ and HR reporters were described elsewhere (42). The NHEJ or HR reporter plasmids were transfected into *iC5*; *C5* KO ESCs, *Cops8* KO, and WT ESCs, and stably integrated clones were established after puromycin selection. A 1- $\mu$ g I-SceI-expressing plasmid was transfected into NHEJ or HR reporter ESC lines to induce a DSB. Forty-eight hours after transfection, cells were harvested for flow cytometry analysis.

**Statistical Analysis.** All data were analyzed by Student's *t* test. Statistically significant *P* values were indicated in figures as follows: \**P* < 0.05; \*\**P* < 0.01; \*\*\**P* < 0.001; \*\*\*\**P* < 0.0001. Averages and SDs of at least three independent experiments are shown in figures when applicable.

**Data Availability Statement.** All data are included in the manuscript and *SI Appendix*.

**ACKNOWLEDGMENTS.** L.C. was supported by the National Key R&D Program of China (Grants 2018YFC1313003 and 2018YFA0107002); the National Natural Science Foundation of China (Grants 31622038, 31671497, and 31871485); the Natural Science Foundation of Tianjin (Grant 18JCQJC48400); the 111 Project Grant (Grant B08011); and the Fundamental Research Funds for the Central Universities.

1. A. Tubbs, A. Nussenzweig, Endogenous DNA damage as a source of genomic instability in cancer. *Cell* **168**, 644–656 (2017).
2. M. K. Zeman, K. A. Cimprich, Causes and consequences of replication stress. *Nat. Cell Biol.* **16**, 2–9 (2014).
3. S. Efroni *et al.*, Global transcription in pluripotent embryonic stem cells. *Cell Stem Cell* **2**, 437–447 (2008).
4. T. Burdon, A. Smith, P. Savatier, Signalling, cell cycle and pluripotency in embryonic stem cells. *Trends Cell Biol.* **12**, 432–438 (2002).
5. R. B. Cervantes, J. R. Stringer, C. Shao, J. A. Tischfield, P. J. Stambrook, Embryonic stem cells and somatic cells differ in mutation frequency and type. *Proc. Natl. Acad. Sci. U.S.A.* **99**, 3586–3590 (2002).
6. X. Fu, K. Cui, Q. Yi, L. Yu, Y. Xu, DNA repair mechanisms in embryonic stem cells. *Cell. Mol. Life Sci.* **74**, 487–493 (2017).
7. I. Vitale, G. Manic, R. De Maria, G. Kroemer, L. Galluzzi, DNA damage in stem cells. *Mol. Cell* **66**, 306–319 (2017).
8. G. Saretzki *et al.*, Downregulation of multiple stress defense mechanisms during differentiation of human embryonic stem cells. *Stem Cells* **26**, 455–464 (2008).
9. S. Maynard *et al.*, Human embryonic stem cells have enhanced repair of multiple forms of DNA damage. *Stem Cells* **26**, 2266–2274 (2008).
10. E. D. Tichy *et al.*, Mouse embryonic stem cells, but not somatic cells, predominantly use homologous recombination to repair double-strand DNA breaks. *Stem Cells Dev.* **19**, 1699–1711 (2010).
11. M. Zalzman *et al.*, Zscan4 regulates telomere elongation and genomic stability in ES cells. *Nature* **464**, 858–863 (2010).
12. B. Zhao *et al.*, Fila1 is an ESC-specific regulator of DNA damage response and safeguards genomic stability. *Cell Stem Cell* **16**, 684–698 (2015).
13. J. Xiong *et al.*, Stemness factor Sall4 is required for DNA damage response in embryonic stem cells. *J. Cell Biol.* **208**, 513–520 (2015).
14. G. Saretzki, L. Armstrong, A. Leake, M. Lako, T. von Zglinicki, Stress defense in murine embryonic stem cells is superior to that of various differentiated murine cells. *Stem Cells* **22**, 962–971 (2004).
15. H. Kondoh *et al.*, A high glycolytic flux supports the proliferative potential of murine embryonic stem cells. *Antioxid. Redox Signal.* **9**, 293–299 (2007).
16. N. Shyh-Chang, G. Q. Daley, Metabolic switches linked to pluripotency and embryonic stem cell differentiation. *Cell Metab.* **21**, 349–350 (2015).
17. S. Varum *et al.*, Energy metabolism in human pluripotent stem cells and their differentiated counterparts. *PLoS One* **6**, e20914 (2011).
18. J. Zhang *et al.*, UCP2 regulates energy metabolism and differentiation potential of human pluripotent stem cells. *EMBO J.* **30**, 4860–4873 (2011).
19. S. Lyapina *et al.*, Promotion of NEDD-CUL1 conjugate cleavage by COP9 signalosome. *Science* **292**, 1382–1385 (2001).
20. N. Wei, G. Serino, X. W. Deng, The COP9 signalosome: More than a protease. *Trends Biochem. Sci.* **33**, 592–600 (2008).
21. D. A. Chamovitz, Revisiting the COP9 signalosome as a transcriptional regulator. *EMBO Rep.* **10**, 352–358 (2009).
22. R. Groisman *et al.*, The ubiquitin ligase activity in the DDB2 and CSA complexes is differentially regulated by the COP9 signalosome in response to DNA damage. *Cell* **113**, 357–367 (2003).
23. N. Y. Chia *et al.*, A genome-wide RNAi screen reveals determinants of human embryonic stem cell identity. *Nature* **468**, 316–320 (2010).
24. W. Zhang *et al.*, Cops2 promotes pluripotency maintenance by stabilizing Nanog protein and repressing transcription. *Sci. Rep.* **6**, 26804 (2016).
25. P. Li, N. Ding, W. Zhang, L. Chen, COPS2 antagonizes OCT4 to accelerate the G2/M transition of mouse embryonic stem cells. *Stem Cell Rep.* **11**, 317–324 (2018).
26. K. Tomoda, N. Yoneda-Kato, A. Fukumoto, S. Yamanaka, J. Y. Kato, Multiple functions of Jab1 are required for early embryonic development and growth potential in mice. *J. Biol. Chem.* **279**, 43013–43018 (2004).
27. K. Lykke-Andersen *et al.*, Disruption of the COP9 signalosome Csn2 subunit in mice causes deficient cell proliferation, accumulation of p53 and cyclin E, and early embryonic death. *Mol. Cell. Biol.* **23**, 6790–6797 (2003).
28. S. Menon *et al.*, COP9 signalosome subunit 8 is essential for peripheral T cell homeostasis and antigen receptor-induced entry into the cell cycle from quiescence. *Nat. Immunol.* **8**, 1236–1245 (2007).
29. H. Chen *et al.*, Erk signaling is indispensable for genomic stability and self-renewal of mouse embryonic stem cells. *Proc. Natl. Acad. Sci. U.S.A.* **112**, E5936–E5943 (2015).
30. J. Rohozinski, A. I. Agoulnik, H. L. Boettger-Tong, C. E. Bishop, Successful targeting of mouse Y chromosome genes using a site-directed insertion vector. *Genesis* **32**, 1–7 (2002).
31. L. Tian *et al.*, Essential roles of Jab1 in cell survival, spontaneous DNA damage and DNA repair. *Oncogene* **29**, 6125–6137 (2010).
32. H. de Waard *et al.*, Cell-type-specific consequences of nucleotide excision repair deficiencies: Embryonic stem cells versus fibroblasts. *DNA Repair (Amst.)* **7**, 1659–1669 (2008).
33. A. Bahat *et al.*, MTCH2-mediated mitochondrial fusion drives exit from naïve pluripotency in embryonic stem cells. *Nat. Commun.* **9**, 5132 (2018).
34. L. Buzaglo-Azriel *et al.*, Loss of muscle MTCH2 increases whole-body energy utilization and protects from diet-induced obesity. *Cell Rep.* **14**, 1602–1610 (2016).
35. M. Maryanovich *et al.*, An MTCH2 pathway repressing mitochondria metabolism regulates haematopoietic stem cell fate. *Nat. Commun.* **6**, 7901 (2015).
36. K. Yamano, N. Matsuda, K. Tanaka, The ubiquitin signal and autophagy: An orchestrated dance leading to mitochondrial degradation. *EMBO Rep.* **17**, 300–316 (2016).
37. A. Khaminets, C. Behl, I. Dikic, Ubiquitin-dependent and independent signals in selective autophagy. *Trends Cell Biol.* **26**, 6–16 (2016).
38. D. Yang *et al.*, COPS5 negatively regulates goat endometrial function via the ERN1 and mTOR-autophagy pathways during early pregnancy. *J. Cell. Physiol.* **234**, 18666–18678 (2019).
39. P. P. Naik, A. Birbrair, S. K. Bhutia, Mitophagy-driven metabolic switch reprograms stem cell fate. *Cell. Mol. Life Sci.* **76**, 27–43 (2019).
40. A. Vazquez-Martin *et al.*, Mitophagy-driven mitochondrial rejuvenation regulates stem cell fate. *Aging (Albany N.Y.)* **8**, 1330–1352 (2016).
41. S. Limsirichaikul *et al.*, A rapid non-radioactive technique for measurement of repair synthesis in primary human fibroblasts by incorporation of ethynyl deoxyuridine (EdU). *Nucleic Acids Res.* **37**, e31 (2009).
42. Z. Mao, M. Bozzella, A. Seluanov, V. Gorbunova, Comparison of nonhomologous end joining and homologous recombination in human cells. *DNA Repair (Amst.)* **7**, 1765–1771 (2008).